Colloid Polym Sci (2014) 292:599–612
DOI 10.1007/s00396-013-3102-y

ORIGINAL CONTRIBUTION

Cross-linked starch nanoparticles stabilized Pickering emulsion polymerization of styrene in w/o/w system

Nasser Nikfarjam · Nader Taheri Qazvini · Yulin Deng

Received: 31 August 2013 / Revised: 11 October 2013 / Accepted: 18 October 2013 / Published online: 10 November 2013
© Springer-Verlag Berlin Heidelberg 2013

Abstract Here, we present a method to synthesize expandable spherical polystyrene beads containing well-dispersed water microdroplets. The beads, 2–3 mm in diameter, were prepared through surfactant-free Pickering emulsion polymerization in water-in-oil-in-water (w/o/w) system using cross-linked starch nanoparticles (CSTN) as emulsifier. The CSTNs were in situ surface-modified by styrene maleic anhydride copolymer as confirmed by infrared spectroscopy and contact angle analysis. The entrapped water microdroplets with the average size of 3–4 μm were shown to be surrounded by a dense layer of the CSTN. The number droplet density as well as water encapsulation efficiency in the polystyrene beads increased with the CSTN concentration. Furthermore, regardless of CSTN content, all samples exhibited high encapsulation stability of over 68 % after 3 months. These characteristics along with good expansion behavior suggest the synthesized beads as expandable polystyrene containing water as a green blowing agent.

Keywords Water expandable polystyrene · Inverse Pickering emulsion polymerization · Starch nanoparticle · w/o/w emulsion · Droplet size distribution

N. Nikfarjam · N. Taheri Qazvini (✉)
Polymer Division, School of Chemistry, College of Science, University of Tehran, Tehran, Iran
e-mail: ntaheri@hsph.harvard.edu

N. Nikfarjam · Y. Deng (✉)
School of Chemical and Biomolecular Engineering, Georgia Institute of Technology, Atlanta, GA, USA
e-mail: Yulin.deng@ipst.gatech.edu

Present Address:
N. Taheri Qazvini
School of Public Health, Harvard University, Boston, MA, USA

Introduction

Basically, emulsions are well known as thermodynamically unstable systems. They are kinetically stabilized by addition of solid particles and surfactants or a mixture of surfactant with other amphiphilic polymers. When solid particles are used to stabilize an emulsion, the process is referred to as a Pickering emulsion [1]. Solid particles as stabilizer can reside at the oil/water interface and promote droplet stability. Depending on the emulsion type, oil-in-water (o/w) or water-in-oil (w/o), the mechanism of emulsion stabilization by solid particles is completely different. For o/w emulsions, of which the contact angle (θ) of colloidal particles is needed to be less than 90°, the particles form a densely close-packed film (monolayer or more than one layer) around the droplets due to particle–particle interaction. Under this condition, the crust film can sterically inhibit the coalescence of emulsion droplets [2–4]. In contrast, the particles with $\theta > 90°$ tend to develop a w/o emulsion by bridging stabilization mechanism suggested by Horozov and Binks [5]. They proposed that the emulsion droplets that sparsely covered with strongly repulsive particles are then stabilized via the formation of a dense bridging monolayer [5].

Different types of solid stabilizers including organic and inorganic materials have been used to produce stable emulsions. Recently, there is a great interest in using of natural polymers like starch as stabilizer to prepare Pickering emulsions [6–12]. As an abundant and cheap biopolymer, starch granules of various size, shape, and composition can be obtained from a wide range of natural sources. The hydrophilic nature of starch granules decreases their affinity to the oil–water interface. Therefore, the native starch granules cannot be directly used for w/o emulsification. The hydrophilicity can be decreased via chemical or physical modifications. For instance, octenyl succinic anhydride (OSA) is commonly used for chemical hydrophobization of starch. OSA modified starch granules of 1–5 μm in size have been used as emulsifier and stabilizer to

prepare o/w emulsions with various droplet sizes commonly between 10 and 100 μm [6–10]. Water-in-oil-in-water (w/o/w) emulsions were also prepared using PGPR90 as lipophilic surfactant and OSA modified starch as relatively hydrophilic emulsifier [11]. Furthermore, starch nanocrystals of around 100 nm in diameter [12] and uniform starch nanospheres modified by OSA [13] have also been used as emulsifier to prepare o/w emulsions with a droplet size distribution of 10–50 μm. In general, despite of large droplet size of emulsions prepared by starch particles, the obtained emulsions were coalescence resistant, i.e., were stable over months [7, 10, 12].

Moreover, several researchers have put efforts into polymerization of oil phase of inverse emulsions (referred to as inverse emulsion polymerization), which are stabilized by common surfactants or by solid particles and mainly surfactant molecules to provide the system with colloidal stability. Nonionic surfactants like Span 80 or anionic surfactants such as sodium bis-2-ethylhexylsulfosuccinate (AOT) are commonly used in inverse emulsion polymerization [14, 15]. Likewise, Cloisite 20A, Laponite, and SiO_2 have been used in surfactant-free inverse Pickering emulsion polymerization [16–20].

Crevecoeur et al. [21] took a further step forward and polymerized styrene in a double emulsion system with the purpose of entrapping water droplets inside polystyrene matrix for the preparation of expanded polystyrene (EPS) beads. The presence of water as small droplet inside polystyrene matrix serves as the green blowing agent. However, unlike organic blowing agent such as pentane, water is absolutely immiscible with PS. Therefore, it is difficult to prepare EPS with encapsulated water droplets as the blowing agent using traditional emulsion polymerization method. Instead, an alternative route, such as inverse emulsion polymerization, should be exploited [21–24].

To achieve a good expandability, it is necessary to reach a fine and uniform dispersion of water droplets inside the PS matrix. Furthermore, in order to preserve the expandability after storage, the water droplets should be highly stabilized inside the beads. Despite several attempts to synthesize water expansible polystyrene beads [21–26], the preservation of the trapped water over time is still a big challenge. Here, we propose that the Pickering emulsion polymerization might be a good way to cope with this problem. As the emulsions prepared by solid particles can be more stable than those prepared by synthetic surfactants [27].

In the following, we first describe the preparation of cross-linked starch nanoparticle (CSTN), then the preparation of water/styrene/water emulsion using CSTN as inverse emulsion emulsifier, and finally the polymerization of styrene to obtain polystyrene beads containing uniformly dispersed fine water droplets. The effect of CSTN content on emulsified water as well as the size, density, and distribution of water droplets are explained based on thermogravimetry analysis (TGA) and field emission scanning electron microscopy (FE-SEM). In this study, the cross-linked starch nanoparticles are used directly, and they are in situ surface-modified during the polymerization. The modified CSTNs are isolated from the obtained beads and the grafting mechanism are investigated and proven by Fourier-transform infrared spectroscopy (FT-IR) and contact angle analysis. Finally, we discuss that the water inside the PS beads is quite stable and therefore can be served as a green blowing agent.

Experimental

Materials

Unmodified cornstarch was provided by National Starch and Chemical Co. (USA). Styrene and maleic anhydride were obtained from Aldrich. Hydroxyethyl cellulose (HEC, Mw~ 250,000 g mol^{-1}) as suspension stabilizer was obtained from Fluka. Benzoyl peroxide 97 % (half-life at 90 °C of 145 min) was supplied by Alfa Aesar. Toluene, ethanol, and citric acid were supplied by Merck. All reagents were used without further purification. Distilled water was used for all experiments.

Synthesis of cross-linked starch nanoparticle

Cross-linked starch nanoparticles were fabricated according to Ma et al.'s method [28]. Briefly, cornstarch was added into distilled water and gelatinized completely at 90 °C for 1 h. The temperature was set at 70 °C and then ethanol, three times of the amount of water used for starch gelatinization, was added dropwise to the gelatinized starch solution with constant stirring. The suspensions were centrifuged and the settled starch nanoparticles (STNs) were washed using ethanol to remove the water. After complete washing, the STNs were dried at 50 °C to remove ethanol. The appropriate amount of solution of citric acid in ethanol (60 % W/W_{starch}) were added to STNs in a glass tray and conditioned for 12 h at room temperature to allow the absorption of citric acid solution by STNs. The tray was dried in vacuum oven to remove ethanol. The obtained material was ground and dried in a forced air oven for 1.5 h at 130 °C. The dried powder was washed three times with water to remove unreacted citric acid. CSTNs were finally washed with ethanol to remove water, dried at room temperature, and ground. The dried STNs and CSTNs were used for testing.

Synthesis of polystyrene beads in w/o/w double emulsion system

To obtain a fine dispersion of CSTN particles in water, a defined amount of CSTN (Table 1) in 7.5 ml of water was stirred at room temperature for 24 h and then at 80 °C for 4 h. The dispersion was then sonicated (Heat system ultrasonic W-385, power 50 %, frequency 1s) for 5 min.

The synthesis of the beads started with dissolution of maleic anhydride and benzoyl peroxide in styrene (Table 1). The

Table 1 Suspension polymerization recipe

Component	Content (g)
Styrene	50-*K*[a]
CSTN[b]	*K*
BPO[b]	(0.5/100)×(50-*K*)
Maleic anhydride	(0.5/100)×(50-*K*)
Water (emulsified)	7.5
Water (suspension)	200
HEC[b]	0.6

[a] *K*, varying 0, 0.25, 0.5, 1, 1.5 g

[b] *CSTN* cross-linked nanostarch, *BPO* benzoyl peroxide, and *HEC* hydroxyethyl cellulose

mixture was heated to 90 °C and polymerized in the bulk for 75 min up to a conversion of around 25 % (determined by gravimetrical method) while stirring at 300 rpm under nitrogen atmosphere. Subsequently, water (15 wt.% based on total content) containing 0, 0.25, 0.5, 1, 1.5 g of CSTN (corresponding to 0, 0.5, 1, 2, 3 wt.% of CSTN) was added to the pre-polymerized styrene. The mixture was then emulsified by stirring vigorously at 800 rpm at 90 °C for 2 min. Due to high viscosity of CSTN aqueous solutions, the systems containing more than 3 wt.% of CSTN did not give a stable inverse emulsion and phase separated in inverse emulsion preparing step. Then, to reach a fine dispersion of all the components in the styrenic phase, the mixture was sonicated again for 4 min. The inverse emulsion was afterwards transferred quickly to a 500-ml glass reactor equipped with mechanical stirrer containing water and HEC as given in Table 1. The suspension polymerization was continued 18 h at 90 °C in a nitrogen atmosphere while stirring at 500 rpm. Finally, the suspension was cooled to room temperature and the white and shiny spherical beads were filtered and washed with water several times (Fig. 1). The reaction mixture/suspension media was 1/4 (w/w) for all suspension polymerizations.

Fractionation of the polystyrene beads

To study the in situ modification mechanism, the grafted CSTN was separated from the polymer matrix via the following fractionation procedure: 8 g of the dried final product was dissolved in 400 ml of toluene at room temperature and stirred overnight. The dispersion was then separated by centrifugation at 8,000 rpm for 1 h. To remove the remaining ungrafted polymer matrix from the grafted CSTN (modified CSTN), the separated solid content was extracted in the Soxhlet extractor for 72 h with toluene. The obtained grafted CSTN was dried to the constant weight and characterized by FT-IR and contact angle analysis before and after grafting.

Thermogravimetric analysis

To determine the emulsified water content of the beads right after synthesis and after 1 and 3 months, the weight loss was measured using a PerkinElmer STA6000 under an N_2 flow of 20 ml min^{-1} and the heating rate of 20 °C min^{-1} from 30 to 600 °C.

Field emission scanning electron microscopy

Native corn starch granules was set on a clean glass slide and then vacuum-coated with gold. The CSTNs were dispersed into water using sonication for 5 min. The dispersion were then applied on a glass slide, dried, and then vacuum-coated with gold. The compact and expanded PS beads were also cut by a razor blade and subsequently were coated with a gold layer. Digital images of the samples were acquired with the Hitachi S4160 field emission scanning electron microscope operating at 20 kV.

Fourier-transform infrared spectroscopy

Synthesized CSTN, the native starch, STN, and the modified CSTN recovered after fractionation process were characterized by FT-IR spectroscopy (BRUKER, EQUNIX 55 spectrophotometer, Germany) from 450 to 4,000 cm^{-1}.

X-ray diffraction

X'pert pro Alpha-1 diffractometer (PANalytical B.V., Netherlands) operated at the Cu-Kα wavelength of 1.54056 Å were used. Cornstarch, STN, and CSTN powders were tightly packed into the sample holder. X-ray diffraction patterns were recorded in the reflection mode in angular (2θ) range of 5–40° at ambient temperature and in 0.01° steps, 0.5 s per step. Powders were dried at room temperature for 4 days prior to analysis.

Contact angle

The CSTN film was prepared by spreading CSTN in ethanol dispersion on a clean glass slide letting the ethanol evaporate at room temperature. To prepare modified CSTN film, the obtained dried modified CSTN was dissolved in toluene overnight, and then placed on a clean glass slide droplet by droplet. The both films were quite smooth. The contact angle was determined with deionized water, using Shen Jun An color camera (SJA-833) and ImageJ2x software. Three readings were taken on each sample in order to obtain an average over the heterogeneity of the surfaces. The films were placed in a vacuum oven at 50 °C for 4 h before measurements.

Results and discussion

Characterization of the synthesized CSTN

FT-IR

Figure 2a shows the FT-IR spectra of cornstarch, STN, and CSTN powders. The characteristic peak occurred at 1, 647 cm^{-1}, which is believed to be a feature of tightly bound

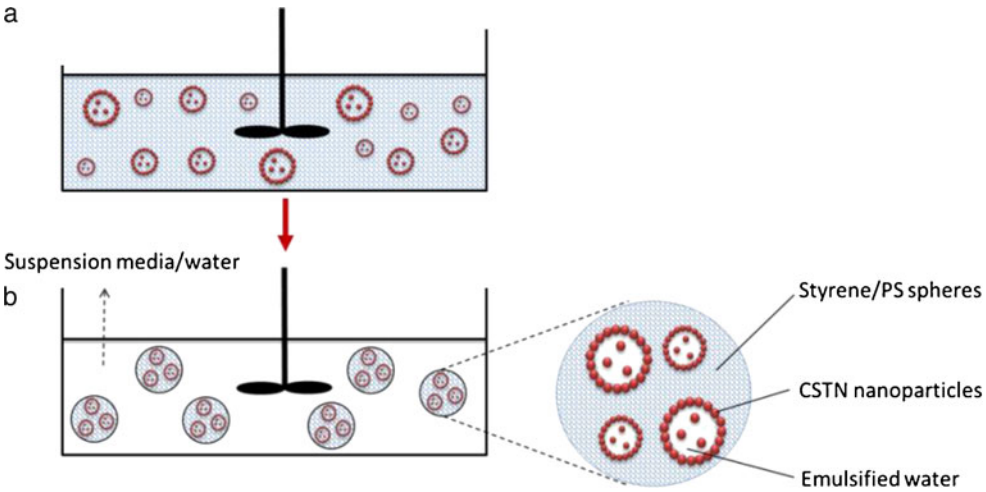

Fig. 1 Schematic representation of the preparation process of the beads in w/o/w system. **a** Emulsification of water in pre-polymerized styrene mixture using CSTN particles, and **b** suspension polymerization of styrene/PS droplets containing emulsified water

water present in the starch [29]. The absorption bands between 1,000 and 1,200 cm^{-1} were characteristics of the -C-O- stretching on polysaccharide skeleton. Cornstarch and STN exhibited similar FT-IR spectra. When citric acid is heated alone, it dehydrated and yielded an anhydride; where it was heated in the presence of starch, a cross-linked starch–citrate derivative was obtained (Fig. 2c). Further heating results in additional dehydration with cross-linking [30]. For CSTN powders, a new peak at 1,725 cm^{-1} is characteristic of an ester group. The other peak at 1,017 cm^{-1} is attributed to C-O bond stretching of the C-O-C group in the anhydroglucose ring. In cornstarch and STN, the oxygen of the C-O-C group

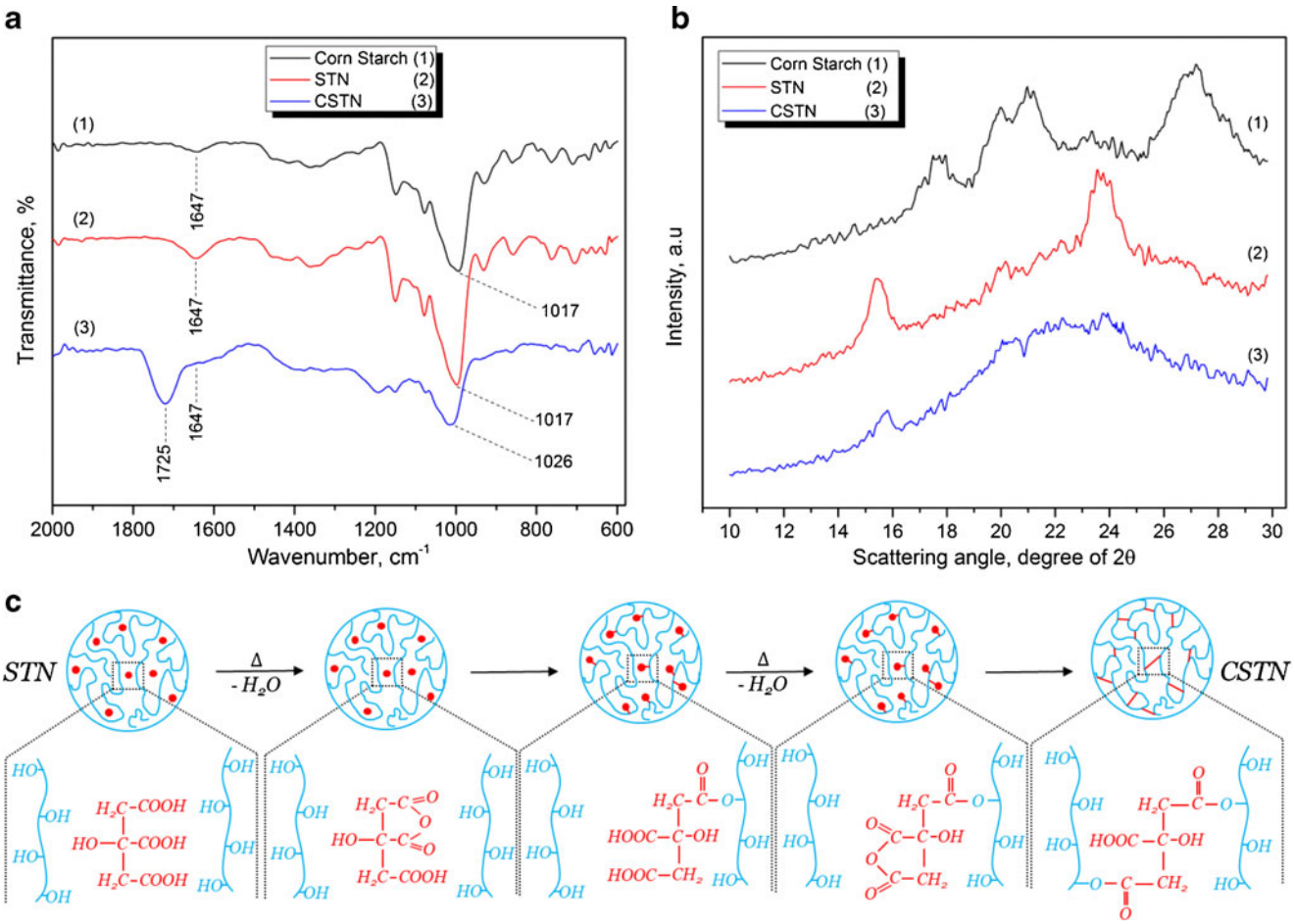

Fig. 2 **a** FT-IR spectra of corn starch (*1*), STN (*2*), and CSTN (*3*). **b** X-ray diffractograms of corn starch (*1*), STN (*2*), and CSTN powders (*3*). **c** Reaction scheme of citric acid with STN for preparing CSTN

could form the hydrogen-bond interaction with the hydrogen of hydroxyl groups, while the ester bonds in the CSTN sterically hinder this hydrogen-bond interaction. The weakening of this interaction shifts the C-O bond stretching of the C-O-C group to 1,026 cm^{-1} [31].

X-ray diffraction

Native cornstarch showed an A-type crystalline structure, a close-packed arrangement with water molecules between each double-helical structure, with major reflections at $2\theta = 15.3$ and 23.4°, and an unresolved doublet at 17 and 18° (Fig. 2b-1). In STN, however, the V_H-type crystalline structure could originate from a single-helical structure "inclusion complex" made up of amylose and substances, here ethanol [32]. The similar V_H-type structure has also reported for the plasticized cornstarch [33]. When ethanol was gradually delivered to the starch-paste solution, gelatinized starch nanoparticles were precipitated. The gelatinization destroys A-type structure of cornstarch [34], and therefore the STN exhibits the V_H-type crystalline structure (Fig. 2b-2). In addition, the X-ray pattern of CSTN showed that the most of crystalline structure of the CSTN has disappeared (Fig. 2b-3). When citric acid penetrated into the STNs through channels and cavities, it could disrupt the V_H-type crystalline structure of starch. The reaction occurs both in the amorphous and crystalline phases [35].

Scanning electron microscopy

The CSTNs are spherical particles with uniform size distribution centered at 250 nm (Fig. 3). Substitution of citric acid groups on starch chains could form a highly cross-linked starch, and thus the CSTNs are very stable against severe conditions of ultrasound waves and polymerization. Scanning electron microscopy on the beads before and after expansion (not shown here) revealed that due to high cross-linking density, the CSTNs remained unchanged in shape and size after polymerization and expansion.

Preparation of water included polystyrene beads in w/o/w system

In order to emulsify water in PS matrix as fine and well-dispersed droplets, the aqueous dispersion of CSTN was added to the pre-polymerized styrene/PS mixture, under mechanical agitation (800 rpm/min) (Fig. 1a). Then, the mixture was suspended in water containing suspension stabilizer (Fig. 1b). The size of final beads varied between 2 and 3 mm. In the emulsification step (Fig. 1a), an optimized viscosity of the styrene phase was needed to prevent the aggregation of CSTNs and to fixate the water droplets in styrene/PS phase. High viscosity of the styrene phase can also prevent the washing-out of CSTNs from styrene phase to suspension water. The optimized viscosity was achieved by partially pre-polymerization of styrene up to the conversion of ~25 %.

Furthermore, to compatibilize CSTNs with PS matrix, an optimized amount of maleic anhydride, 0.5 wt.% relative to styrene content, was added to the formulation. During the pre-polymerization step, maleic anhydride copolymerizes with styrene and produces poly(styrene-co-maleic anhydride) (SMA) in different molecular weights and maleic anhydride contents [25, 36]. It was proposed that the obtained SMA copolymer can react with the hydroxyl groups on the CSTN surface and change the nature of CSTN from hydrophilic to relatively hydrophobic. Consequently, the modified CSTNs could locate on the water/oil interface and therefore stabilize water droplets in styrenic phase [25, 36]. The modification process and its mechanism will be discussed in greater detail later and it will be shown that the CSTN is truly grafted with SMA.

Basic features of double emulsion samples

The amount of emulsified water in the beads was evaluated from TGA results. The emulsified water increases with the increase in CSTN concentration (Table 2). Almost all studies conducted on particle-stabilized emulsions have shown that with increasing particle concentration, the emulsion volume

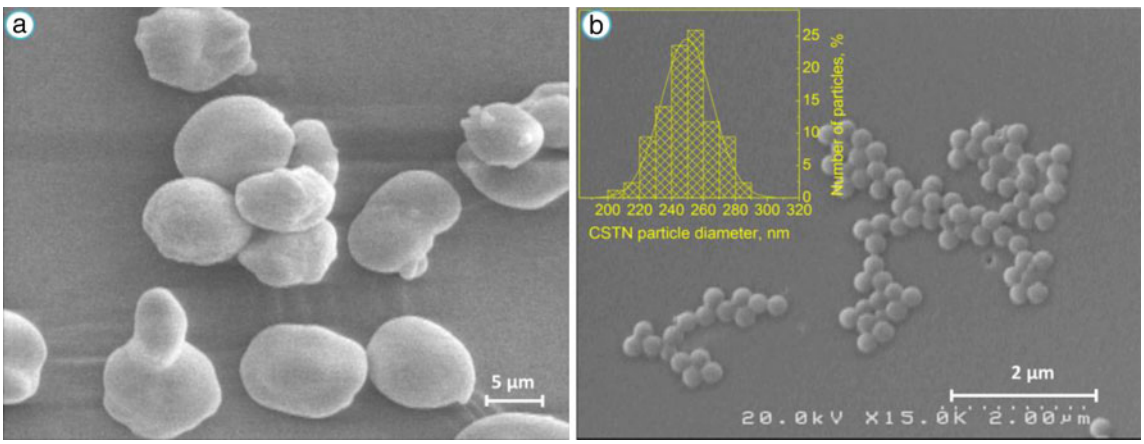

Fig. 3 FE-SEM micrographs of **a** cornstarch granules and **b** CST nanoparticles. The CSTNs have a narrow size distribution centered at 250 nm

Table 2 Characteristics of the prepared PS bead samples with different CSTN amounts as emulsion stabilizer

Sample	CSTN (wt.%)	Water content (wt.%)	Water droplet number density (N_0), (#/mm^3)	Encapsulation efficiency (EE %)	Average droplet size ($d_{4,3}$) (μm)
Sample-0	0	3.22	–	–	–
Sample-0.5	0.5	5.01	3.9×10^4	33.4	4.0±0.2
Sample-1	1	5.62	8.6×10^4	37.5	3.0±0.1
Sample-2	2	10.10	1.8×10^5	67.3	3.1±0.1
Sample-3	3	11.90	2.4×10^5	79.3	3.0±0.1

*Based on total content

would increase [11, 37]. Obviously, when there is more emulsifier in the system, the number of water droplets and therefore total water content increases. The morphology of the beads was studied by FE-SEM (Fig. 4) and the droplet number density was estimated by the following equation:

$$N_o = \left[\frac{n}{A}\right]^{3/2} \quad (1)$$

Where n is the number of droplets in the defined area A, derived from the SEM micrographs at a magnification of ×600. The number of droplets was manually counted using JMicroVision 1.2.7 software. For each sample, at least 300 droplets were analyzed. The reported values for droplet size are the averages taken 3–4 different analysis runs.

Encapsulation efficiency (EE%), the amount of internal aqueous phase that preserves after emulsification, was calculated by dividing the total trapped water in the bead to the initial water used for emulsification, i.e., 15 wt.% (Table 1). The number density of the droplets as well as the encapsulation efficiency increases with the increase in the CSTN concentration (Table 2) mainly due to the increase in the number of effective CSTNs that stabilize the water droplets. Encapsulation stability (ES %) which quantifies how much of the original encapsulated amount of aqueous phase remains during storage was determined by TGA analysis. The calculated data for the sample 0.5, for example, showed that the residual water after 1 and 3 months was 83.5 and 68.2 % of initial encapsulated water, respectively. In comparison with the residual water 3 months after synthesis (2.63 %) that has been reported for water expandable PS beads prepared using AOT as surfactant and hydrophilic clay nanoparticles [23], our samples offering a very good encapsulation stability. The relatively hydrophilic nature of the CSTNs facilitates the fixation of water within the beads during storage.

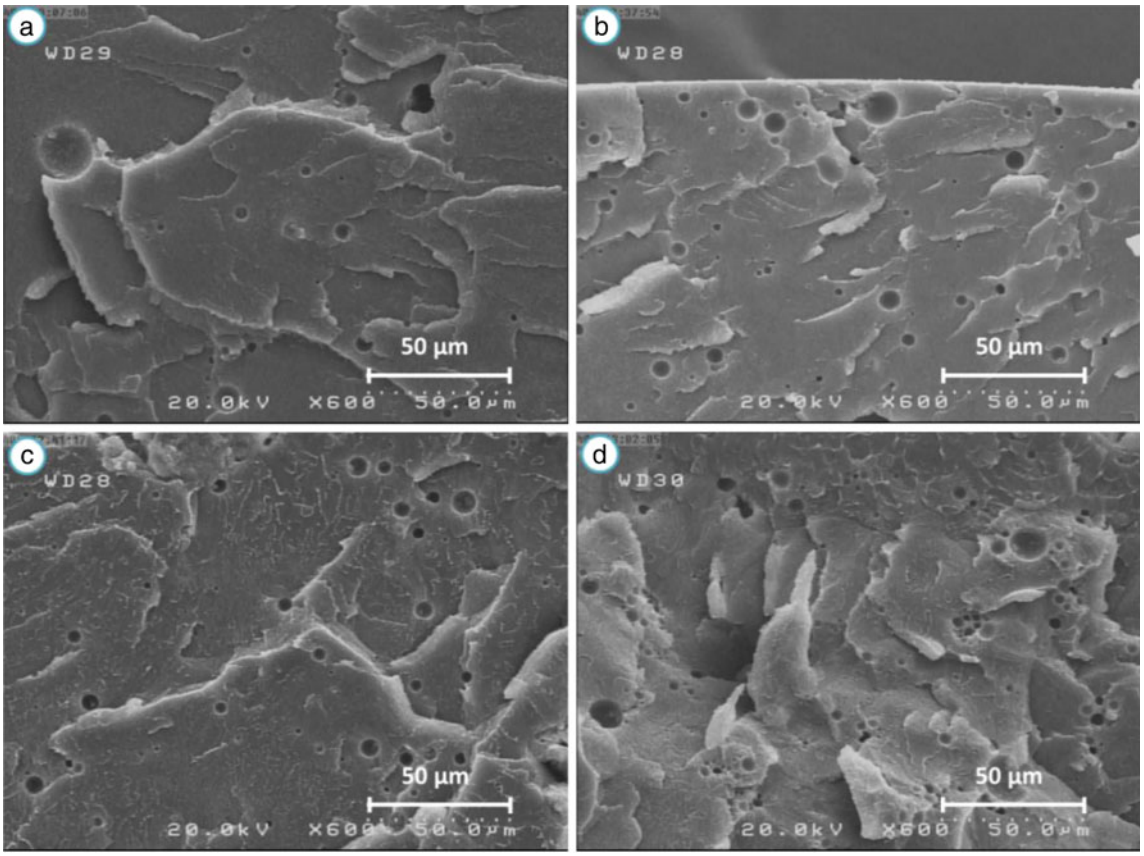

Fig. 4 Cross-section FE-SEM micrographs of the prepared samples with different CSTN contents (*scale bar*=50 μm). **a** sample-0.5, **b** sample-1, **c** sample-2, **d** sample-3

Water droplets morphology

In Pickering emulsions, the droplets are covered with layers of solid particles. The performance of these layers in stabilizing the emulsion depends on the concentration and properties of particles, such as size, shape, inter-particle interactions, and wettability [38]. It is well recognized that the small particles have better ability to form emulsions with smaller droplets and higher stability, due to their high coverage ability.

While the unmodified, uncross-linked starch nanoparticles tend to create o/w emulsion, slightly hydrophobic CSTNs are suitable for w/o emulsion preparation [12]. The cross-linked starch solid nanoparticles can reside at the water–styrene/PS interface and form a dense structure around droplets. The in situ surface modification of the CSTNs by SMA during polymerization gives them a sufficient wettability to stabilize the emulsion as well as sufficient compatibility with the PS matrix.

The FE-SEM micrographs in Fig. 5a, b show the cross-section of water droplets location in the bead and Fig. 5c the details in the inside wall. The spherical particles inside the cavities are attributed to unmodified CSTNs that entered to the droplets, in dispersed water phase, during the emulsion process due to their inherent hydrophilic properties. The protruding spots on the wall inside of the cavities are related to the modified CSTNs which form a wall and finally stabilize the water droplets. Each water droplet is surrounded by a dense layer of CSTNs.

Here in our study, despite the contact angle of modified CSTN is greater than 90° (115°, see Sect. 3.5), the particles can be arranged around droplets in close-packed form (Fig. 5). The reason lies in the fact that surface of the particles has not been entirely modified and therefore there are still some hydroxyl functional groups. This makes the particle–particle interaction via hydrogen bonding possible.

In situ modification of CSTNs

As a natural hydrophilic polymer, starch is immiscible with most of synthetic polymers. This immiscibility can lead to the agglomeration of the CSTNs in polystyrene matrix and to poor performance of the final products. Furthermore, due to the hydrophilicity of CSTN particles, they can be washed-out from the polymerization system. An alternative to cope with this problem is the introduction of polar functional groups like anhydride, epoxy, or carboxylic acid in the polystyrene chain [39]. This causes a positive interaction, and hence a good compatibility between the two components. From the reactivity viewpoint, it is well recognized that cyclic anhydride groups

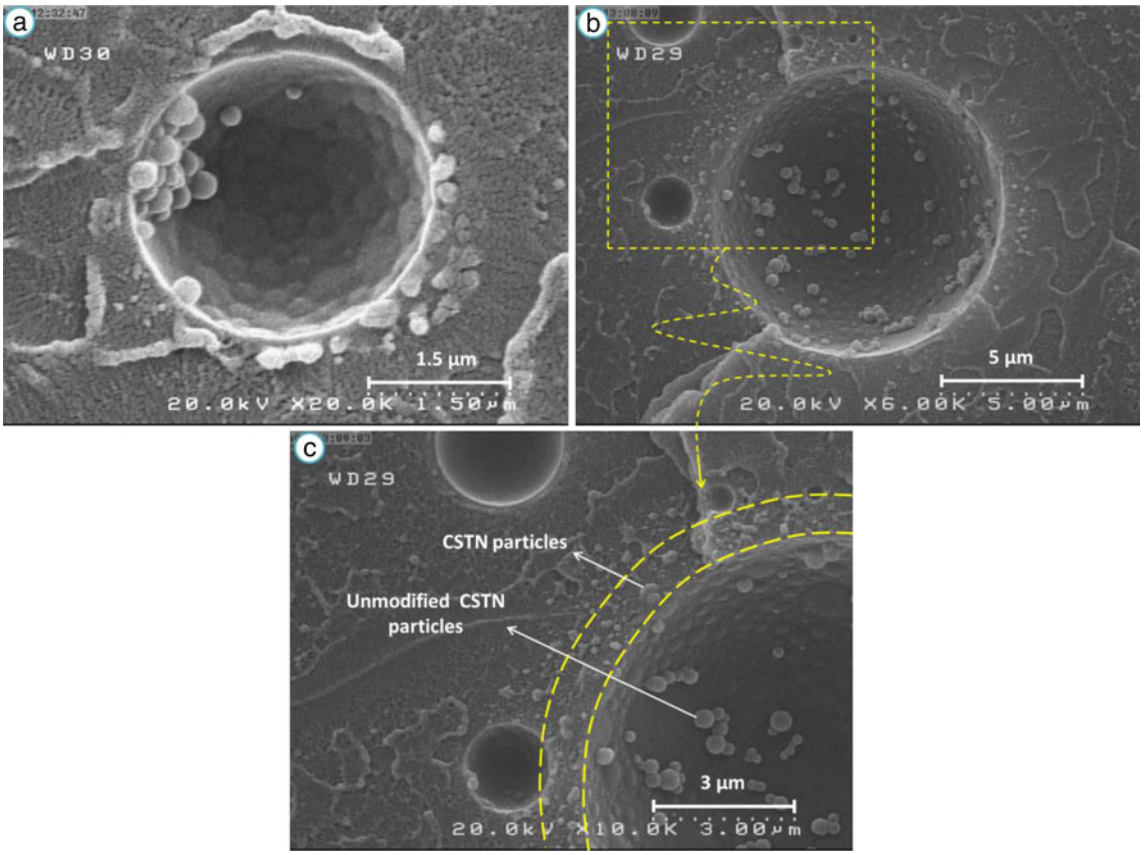

Fig. 5 FE-SEM micrographs of sample-0.5 (**a**) and (**b**) cross-section of a water droplet location in the beads (**c**) The image of interior wall at larger magnification. The modified CSTNs reside at the interface and physically stabilize the emulsion; unmodified CSTNs are located inside the droplets in water phase

react quickly than the other functional groups. For this reason, in this study, maleic anhydride in optimized concentration, 0.5 wt.% relative to styrene, was added to the pre-polymerized styrene mixture. Maleic anhydride copolymerizes with styrene to produce SMA in various molecular weights and maleic anhydride contents [36]. SMA can be grafted on CSTN particles to compatibilize them with PS matrix. This grafting can be ascribed to the reaction (ester) or interaction (hydrogen bonding) of the cyclic anhydride groups in the copolymer with hydroxyl and carboxyl groups of the starch chains or in other words, clearly, CSTN particles (Fig. 6a) [36].

To verify the in situ modification, the modified CSTNs were isolated from the polymer matrix by fractionation process described in the experimental section. The FT-IR spectra of the CSTNs and the grafted CSTNs in the extended range of 600–2, 000 cm^{-1} are shown in Fig. 6b for comparison. In the case of the SMA-grafted CSTNs, the bands at 1,853 and 1,773 cm^{-1} can be assigned to the cyclic anhydride group (C=O) and the bands at 1,157, 1,443, 1,493, 1,583, 1,601 cm^{-1} to the aromatic ring of styrene in SMA [36, 40].

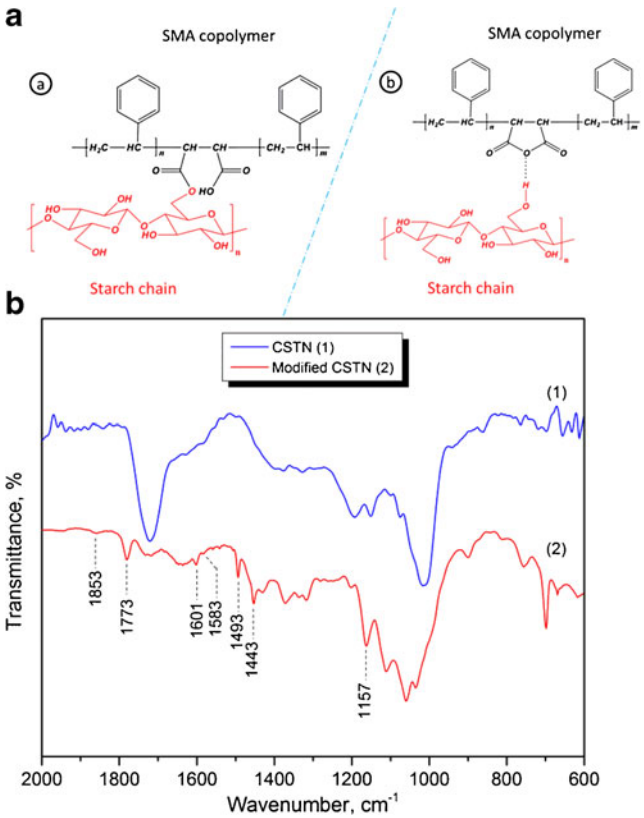

Fig. 6 **a** Maleic anhydride in SMA can modify the surface of CSTN by (1) reaction with the hydroxyl group on the surface of CSTN to form an ester bond and (2) interaction with the hydroxyl group on the surface of CSTN by hydrogen bonding. **b** Extended FT-IR spectrum of CSTN modified by styrene–maleic anhydride copolymer isolated from matrix polymer compared with that of CSTN particles. The peaks at 1,853 and 1,773 cm^{-1} are attributed to maleic anhydride and peaks at 1,157, 1,443, 1,493, 1,583, and 1,601 cm^{-1} show the styrene ring introduced on CSTN

Additional proof of grafting was obtained by contact angle analysis (θ). The measured θ for the CSTN and the modified CSTN were 71±3° and 115±3°, respectively (Fig. 7). In comparison with native cornstarch with a contact angle of 45° [41], this means that the cross-linking by citric acid decrease the hydrophilicity of the starch and the SMA grafting on the CSTNs changes their nature to a hydrophobic material. The average hydrophobicity strongly held the CSTNs at the water–polystyrene interface and leads to fine and stable emulsion droplets.

Water droplets size distribution

The water droplet size distributions (number averages) for the stabilized emulsions in w/o/w system in different amounts of CSTN are shown in Fig. 8. The emulsions exhibit a more complicated distribution behavior. Each distribution, however, has the common feature of a peak with a maximum at around 3 μm. This peak grows with increasing CSTN concentration with a corresponding loss of larger droplets until at the highest concentration a log-normal distribution is achieved. This complicated distribution can be possibly explained using a kinetic argument. During the emulsification, if the droplets fail to acquire enough particles rapidly, coalescence occurs and large emulsion droplets regenerate. For emulsions with viscose continuous phase, the rate of particle diffusion to the droplet surface will be slower. Also more particles are needed at the surface for stability and the thicker crust will be less able to rearrange. As a result, coalescence will occur more readily in this system. Smaller particle-coated droplets have a longer lifetime during the emulsification than the larger droplets. Thus large droplets will tend to coalesce after breakup and small droplets will be stable. And with increasing particle concentration, more small droplets can be stabilized [42]. Therefore, here, the viscose pre-polymerized styrene continuous phase reduces the rate of CSTN particle diffusion and more small water droplets can be stabilized when the CSTN concentration was increased, which explain the observed increase in the peak at droplet diameter around 3 μm (Fig. 8). The lower limit of the droplet size is limited by three factors as follows: the opposing Laplace pressure, which increases with decreasing droplet radius; the mechanical energy supplied during emulsification process; and the ability of the CSTN particles to pack around a droplet of low radius [42].

To better understand overall droplet size variations, the volume-weighted average droplet diameter ($d_{4,3}$) defined by the following equation were calculated (Fig. 9).

$$d_{4,3} = \frac{\sum n_i d_i^4}{\sum n_i d_i^3} \tag{2}$$

Where n_i is the number of particles with diameter d_i. The $d_{4,3}$ value decreases with CSTN concentration. The average

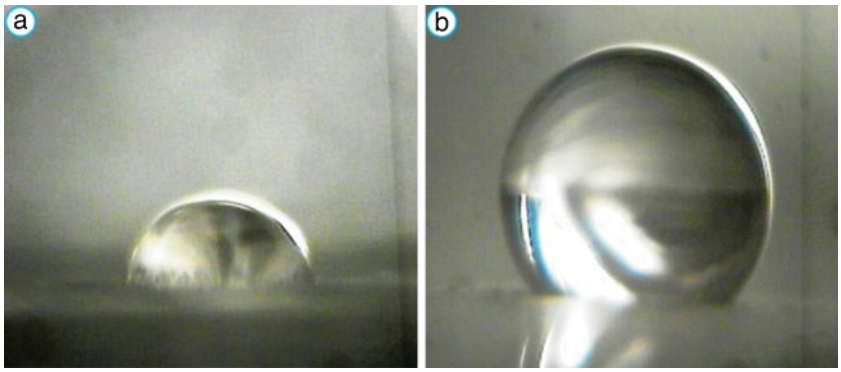

Fig. 7 Deionized water droplet on **a** CSTN film and **b** modified CSTN film

droplet diameter shows a decrease with CSTN concentration (Fig. 9). It has been previously found that the average droplet diameter of solid-stabilized emulsions decreases with particle concentration as more particles are available to stabilize smaller droplets [42–45]. It seems reasonable to assume that, for given emulsification conditions, the phase is broken down initially into droplets in the same extent, irrespective of the particle concentration. Depending on the amount of particles adsorbed on the droplet surfaces, the droplets will coalesce together, reducing the total droplet surface area, until the particle coverage is sufficient to stabilize the droplets against further coalescence.

Unlike other emulsions stabilized by solid particles, in this study, the droplet sizes are so small and droplet size variations occur in a small size range. The major change in size occurs up to 1 wt.% (from 4.03 to 3.02 μm), after which the diameter remains constant (Fig. 9). There are four reasons for the small droplet size. The first is related to the use of ultrasound in preparation of w/o emulsion. It is well known that the average droplet diameter formed using ultrasound is smaller than that of common homogenization methods. Due to higher energy density input, ultrasound waves disrupt the CSTN aggregates in styrenic phase and produce a large number of effective particles to stabilize small droplets. In addition, such disrupted aggregates are then available for immediate adsorption at freshly created oil–water interfaces [46, 47]. The second reason lies on the fact that an increase in the viscosity (η) of continuous phase reduces the diffusion coefficient (D_{diff}) of the droplets. Assuming the Stokes' law is applicable, $D_{diff}=k_BT/6\pi\eta r$, in which k_B is the Boltzmann constant, T is the absolute temperature and r is the radius of the droplets. Smaller diffusion coefficient leads to the lower frequency of the collisions between the droplets as well as to the lower rate of coalescence. Also, sedimentation is suppressed by an increase in viscosity of the continuous phase [48]. And the third reason for the small droplet size is due to the increased viscosity with CSTN particles concentration of the continuous styrenic phase, in which excess particles form a network structure trapping the droplets within [44], and/or connect to continuous phase chains to help improve its viscosity [42, 49]. Furthermore, as the fourth reason, one can think of the direction of migration of CSTNs to the interface. In this study, the CSTNs were initially dispersed in water phase; therefore, during the emulsion preparation, the particles are migrating from the aqueous (dispersed) phase toward the oil–water interface, whereas in other Pickering emulsions, the situation is reversed, i.e., the particles usually migrate from the continuous phase to the oil–water interphase. This helps prevent the kinetic barrier being large.

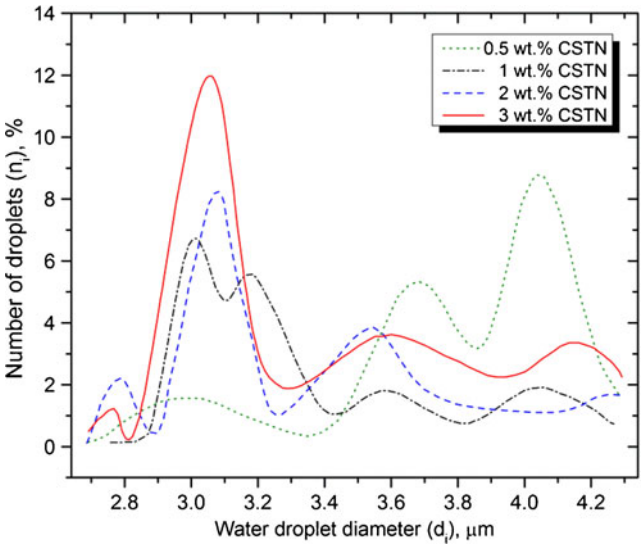

Fig. 8 Effect of CSTN concentration on the water droplet diameter number-based distribution of the emulsion in w/o/w system prepared using different amounts of CSTN

Assuming that the adsorbed particles form a hexagonal close-packed layer on the droplet surface, the number of particles (n_{pa}) required to form a single layer covering the available droplet surfaces can be calculated and compared to the total number of particles available (n_{pt}) (appendix A).

$$n_{pt}/n_{pa} = \left(3\sqrt{3}C\rho_b\right)/\left(8\times10^{-16}N_{\circ}\pi^2\rho_p r_p r_e^2\right) \quad (3)$$

Where C and $N_{\circ}$ are the CSTN content and number density of droplets. r_{e}, r_{p}, ρ_{b}, and ρ_{p} are the radius of droplets (here,

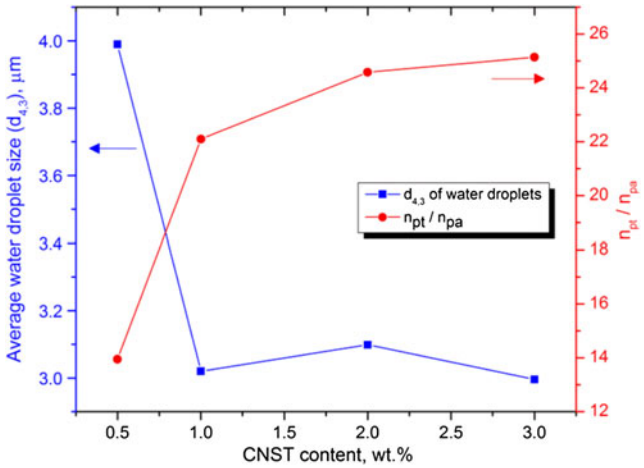

Fig. 9 The variations of the average size ($d_{4,3}$) of water droplets as a function of the CSTN concentration. Also shown is the ratio of the total number of particles available, n_{pt}, to the number required to provide a monolayer around all droplets, n_{pa}

the half of average diameter of droplets ($d_{4,3}$)), the radius of CSTN particle, the density of bead, and the density of CSTN particles, respectively. The required data were presented in Table 2 and r_p, ρ_b, and ρ_p were constant for all samples, and their amount were 250 nm, 1.05 g/cm^3, and 1.2756 g/cm^3, respectively. As discussed previously, the average droplet diameter decreases as the particle concentration increases (Fig. 9). The n_{pt}/n_{pa} ratio rises dramatically with particle concentration (Fig. 9).

Assuming that the all particles are completely used to stabilize droplets, so it is possible to calculate the thickness of particles around a droplet in each sample by the following equation:

$$\left(9\sqrt{2}C\rho_b\right)/\left(4\times10^{-16}N_{\circ}\pi^2\rho_p\right)=(r_e+x)^3+r_e^3 \qquad (4)$$

Where x is the single unknown parameter in Eq. 4 for each sample. The parameter x is attributed to the thickness of particles layer around droplets, in nanometer (appendix B).

To obtain the number of particle layers around the droplets, it was assumed that the droplets are surrounded by particles in an ideal close-packed hexagonal (HCP) structure. The Eq. 5 gives a relation between the particle layer thickness and the numbers of particles layers by considering the height of HCP unit cell (appendix B).

$$L=3x/r_p\left(4\sqrt{(2/3)}+1\right) \qquad (5)$$

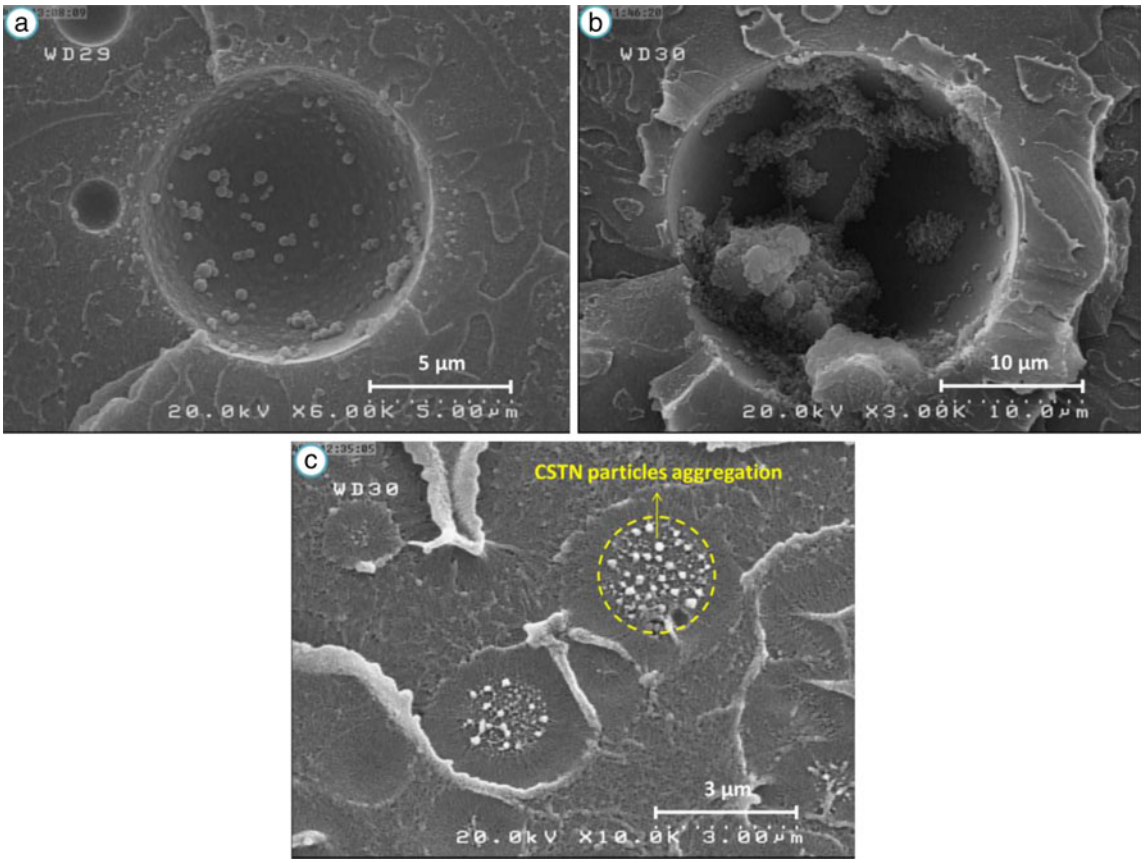

Fig. 10 Cross-section FE-SEM micrographs droplets in **a** sample-0.5 involving 0.5 wt.% of CSTN particles and **b** sample-0.3 involving 0.3 wt.% of CSTN particles; with increase in CSTN content more CSTNs can locate inside of droplets. **c** CSTN particles aggregation in the polystyrene matrix

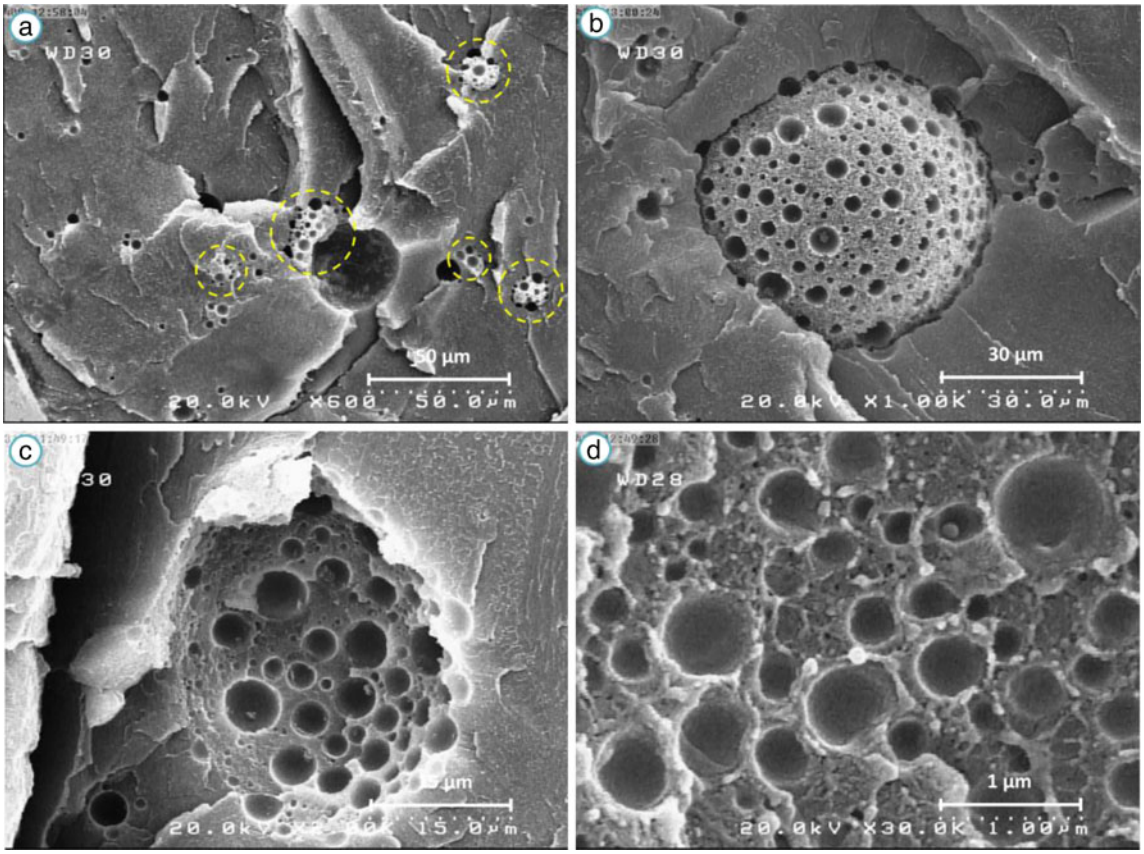

Fig. 11 FE-SEM micrographs for sample-0.3 involving 3 wt.% of CSTN **a** cross-section of prepared bead, the *circles* show the flocculation of droplets in the polystyrene matrix. **b**, **c**, and **d** show the droplet flocculation in more details; in spite of occurring flocculation between droplets, no coalescence was observed

Where L is the number of particle layers that can be existed around droplets. The calculated number of layers were 10.28, 11.57, 11.15, and 12.48 which is corresponding to samples 0.5, 1, 2, and 3, respectively. The calculated data reveals a dense layer of particles around the droplets and the layer is increasingly densely packed as the particle concentration in the emulsion is raised. These observations are consistent with the findings of previous studies by Binks et al. [44, 50]. It is also well consistent with the conclusions drawn from ellipsometric measurements of these particles spread at the planar oil–water interface which showed that the particles tend to adsorb at the interface such that more than a single layer of particles forms at the interface [51]. Due to the attendance of particles inside of water droplet (Fig. 10a, b) and in continuous styrenic phase (Fig. 10c), however, the real number of layers for each sample is likely lower than that of calculated ones.

The effect of the CSTN concentration on the viscosity and the bead morphology

During the emulsification process, the CSTN particles locate in styrenic continuous phase and form 3D network via hydrogen bond interaction between hydroxyl groups of adjacent particles (Fig. 10c). Therefore, it can be concluded that the effective hydrophobicity of the CSTN particles in oil dispersions increases with particle concentration as more and more hydroxyl groups become involved in hydrogen

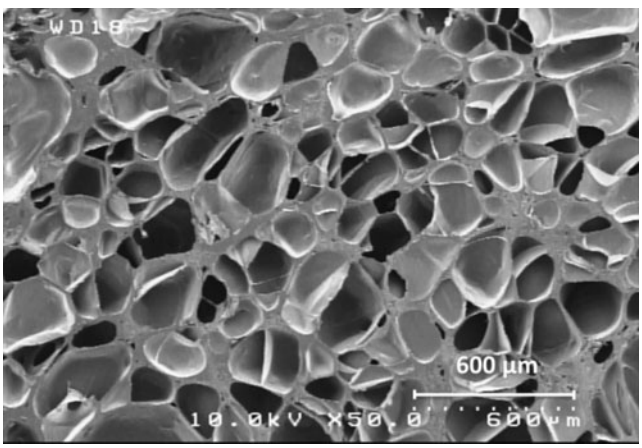

Fig. 12 FE-SEM micrograph of a typical foam morphology of the expanded PS beads prepared via starch nanoparticles stabilized Pickering emulsion polymerization

bonds with each other. In addition, anhydride groups of SMA copolymer in polystyrene matrix can react with hydroxyl groups of CSTN particles and give them a more hydrophobicity to be stabilized well in polystyrene matrix and help to improve the viscosity of matrix. SMA copolymer acts like a coupling agent and resides on CSTN surface to connect them to the matrix or in other words stabilize them in the matrix. These finding are well in agreement with the works done by Raghavan et al. [52] and Binks et al. [45] who studied both w/o and o/w emulsions stabilized by silica particles and measured flow rheology of dispersion of particles possessing SiOH groups in both silicone oil and water as a function of particle concentration. They concluded that the dependence of the viscosity on particle concentration depends on both the hydrophobicity of the particles and the polarity of the liquid. They found that the viscosity of the oil dispersions is always higher than that of aqueous dispersions and the former increase more markedly with particle concentration. As particles aggregate in oil, a volume filling gel forms via hydrogen bonding, whereas such aggregates remain discrete in water. These findings are also in agreement with other studies [42, 52, 53].

The above discussion also explains why in high concentration of CSTN (3 wt.%) the flocculation between the droplets occurs (Fig. 11). This is due to the presence of large number of CSTN particles in matrix which can interact with each other by hydrogen bonding to form a 3D network where water droplets are entrapped in. The yellow circles in Fig. 11a show the droplet flocculation in sample 0.3. In spite of the strong tendency for the droplets to flocculate, no coalescence was observed. Unlike surfactant-stabilized emulsions, the solid particles in Pickering emulsions can form a strong structure at the interface that can sterically and mechanically inhibit the coalescence of emulsion droplets.

Expansion of the PS beads

The PS beads included fine and well-dispersed water droplets are capable of being used as water-blown expandable polystyrene. When the beads are heated at an optimum temperature well above the glass transition temperature of the matrix, the rubbery polystyrene matrix expands as a result of the water vapor pressure developed inside the beads. This forms a foam-like structure with rather regular polyhedral cells (Fig. 12). The beads can be expanded by exposing them to hot oil (optimum temperature of ~135 °C) followed by quenching in cold water. Due to the good dispersion of water microdroplets in the beads, they showed an excellent expansion ratio of around 7. More interestingly, the water droplets inside the polystyrene beads prepared in this study can be reserved over months without adverse effect on the expandability. The expansion behavior of the beads will be addressed in more details elsewhere.

Conclusions

Polystyrene beads containing water droplets in very small sizes were successfully synthesized through surfactant free inverse Pickering emulsion polymerization in w/o/w system using cross-linked starch nanoparticles. The CSTNs were in situ surface-modified by styrene-maleic anhydride copolymer. The modified CSTNs were isolated by fractionation process and their microstructure was characterized by FT-IR and contact angle analysis. It was proposed that the grafting process occurred in two possible forms as follows: esterification and hydrogen bonding between hydroxyl groups on starch macromolecules and cyclic maleic anhydride in SMA chains. In general, the trapped water droplets were fine with the average diameter of 3–4 μm. The water droplets were shown to be surrounded by a dense layer of CSTNs. The thickness of the dense CSTN layer increased as particle concentration was raised. The FE-SEM and thermogravimetric results showed an increase in emulsified water (water encapsulation efficiency) with CSTN concentration. Finally, owing to high encapsulation stability along with good expansion behavior, the beads can be considered as water expandable polystyrene. The expansion behavior of the beads will be reported in more details in a future work

Acknowledgment The authors thank the Institute of Paper Science and Technology (IPST), Georgia Tech for experimental facilities and infrastructure. Rui Zhao, Sudhier Sharma, and Wei Mu in IPST are greatly acknowledged for providing technical support. We also thank the respected reviewers for their helpful comments and suggestions.

Appendix A: calculation of n_{pt}/n_{pa} ratio

The total number of CSTN particle in a defined volume of bead can be calculated from:

$$n_{pt} = (3CV_b\rho_b)/\left(400\pi\rho_p r_p^3\right) \quad \text{(A1)}$$

For water droplets of radius r_e stabilized by CSTN particles of radius r_p, assuming that $r_{e>}r_p$ and that the particles are arranged in a hexagonal close-packed (HCP) arrangement on droplet surfaces and taking the contact angle that the particles make with the oil–water interface equal to 90°, the total number of particles surrounding all droplets in a defined volume of bead (V_b) is as follows:

$$n_{pa} = \left(4N_\circ V_b\pi r_e^2\right)/\left(2\sqrt{3}r_p^2\right) \quad \text{(A2)}$$

Combination of equations A1–A2 leads to the following expression for the total number of particles available to the number of particles required to form a single layer covering the available droplet surfaces.

$$n_{pt}/n_{pa} = \left(3\sqrt{3}C\rho_b\right)/\left(8\times10^{-16}N_\circ\pi^2\rho_p r_p r_e^2\right) \quad \text{(A3)}$$

With C=weight percent of particle (percent), ρ_b= density of bead (grams per cubic meter), ρ_p=density of particle (grams per cubic meter), r_p=radius of particle (nanometers), r_e=radius of droplet (nanometers), and $N_\circ$= number density of droplets (number per cubic millimeter).

Appendix B: calculation of the number of particle layers around the droplets

The following expression is used to find an equation to calculate the thickness of particle layers (x) around the droplets in a defined volume of bead and taking the contact angle that the particles make with the oil–water interface equal to 90°:

$$\frac{\text{total number of particle}}{\text{number of droplets}} = \frac{(\text{volume of particle layers})\times(\text{HCP packing density})}{\text{volume of particle}}$$

This yields

$$\left(9\sqrt{2}C\rho_b\right)/\left(4\times10^{-16}N_\circ\pi^2\rho_p\right) = (r_e+x)^3 + r_e^3 \quad \text{(B1)}$$

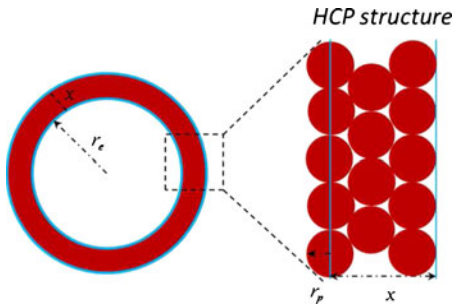

With C=weight percent of particle (percent), ρ_b=density of bead (grams per cubic centimeter), ρ_p=density of particle (grams per cubic centimeter), r_e=radius of droplet (nanometers), $N_\circ$= number density of droplets (numbers per cubic millimeter), and x=thickness of particle layer (nanometers).

With considering the HCP unit cell height and the number of layers in every unit cell, the number of layers around the droplets (L) can be calculated by the following equation:

$$L = 3x/r_p\left(4\sqrt{(2/3)}+1\right) \quad \text{(B2)}$$

References

1. Pickering SU (1907) Journal of the Chemical Society, Transactions 91
2. Tambe DE, Sharma MM (1994) Factors controlling the stability of colloid-stabilized emulsions: II. A model for the rheological properties of colloid-laden interfaces. J Colloid Interface Sci 162(1):1–10. doi:10.1006/jcis.1994.1001
3. Tambe DE, Sharma MM (1995) Factors controlling the stability of colloid-stabilized emulsions: III. Measurement of the rheological properties of colloid-laden interfaces. J Colloid Interface Sci 171(2):456–462. doi:10.1006/jcis.1995.1202
4. Midmore BR (1998) Preparation of a novel silica-stabilized oil/water emulsion. Colloids Surf A Physicochem Eng Asp 132(2–3):257–265. doi:10.1016/S0927-7757(97)00094-0
5. Horozov TS, Binks BP (2006) Particle-stabilized emulsions: A bilayer or a bridging monolayer? Angew Chem Int Ed 45(5):773–776. doi:10.1002/anie.200503131
6. Marku D, Wahlgren M, Rayner M, Sjöö M, Timgren A (2012) Characterization of starch Pickering emulsions for potential applications in topical formulations. Int J Pharm 428(1–2):1–7. doi:10.1016/j.ijpharm.2012.01.031
7. Yusoff A, Murray BS (2011) Modified starch granules as particle-stabilizers of oil-in-water emulsions. Food Hydrocoll 25(1):42–55. doi:10.1016/j.foodhyd.2010.05.004
8. Dokić L, Krstonošić V, Nikolić I (2012) Physicochemical characteristics and stability of oil-in-water emulsions stabilized by OSA starch. Food Hydrocoll 29(1):185–192. doi:10.1016/j.foodhyd.2012.02.008
9. Rayner M, Sjoo M, Timgren A, Dejmek P (2012) Quinoa starch granules as stabilizing particles for production of Pickering emulsions. Faraday Discuss 158:139–155. doi:10.1039/c2fd20038d
10. Timgren A, Rayner M, Sjöö M, Dejmek P (2011) Starch particles for food based Pickering emulsions. Procedia Food Sci 1(0):95–103. doi:10.1016/j.profoo.2011.09.016
11. Matos M, Timgren A, Sjöö M, Dejmek P, Rayner M (2013) Preparation and encapsulation properties of double Pickering emulsions stabilized by quinoa starch granules. Colloids Surf A Physicochem Eng Asp 423(0):147–153. doi:10.1016/j.colsurfa.2013.01.060
12. Li C, Sun P, Yang C (2012) Emulsion stabilized by starch nanocrystals. Starch Stärke 64(6):497–502. doi:10.1002/star.201100178
13. Tan Y, Xu K, Liu C, Li Y, Lu C, Wang P (2012) Fabrication of starch-based nanospheres to stabilize pickering emulsion. Carbohydr Polym 88(4):1358–1363. doi:10.1016/j.carbpol.2012.02.018
14. Xu ZZ, Wang CC, Yang WL, Deng YH, Fu SK (2004) Encapsulation of nanosized magnetic iron oxide by polyacrylamide via inverse miniemulsion polymerization. J Magn Magn Mater 277(1–2):136–143. doi:10.1016/j.jmmm.2003.10.018
15. Ge L, Texter J (2004) Combustion resistant nanocomposites from water/AOT/MMA reverse microemulsions. Polym Bull 52(3–4):297–305. doi:10.1007/s00289-004-0288-7
16. Negrete-Herrera N, Putaux J-L, David L, Bourgeat-Lami E (2006) Polymer/Laponite composite colloids through emulsion polymerization: Influence of the clay modification level on particle morphology. Macromolecules 39(26):9177–9184. doi:10.1021/ma0610515
17. Zhang K, Wu W, Meng H, Guo K, Chen JF (2009) Pickering emulsion polymerization: preparation of polystyrene/nano-SiO2 composite microspheres with core–shell structure. Powder Technol 190(3):393–400. doi:10.1016/j.powtec.2008.08.022

18. Voorn DJ, Ming W, van Herk AM (2006) Polymer–clay nanocomposite latex particles by inverse Pickering emulsion polymerization stabilized with hydrophobic montmorillonite platelets. Macromolecules 39(6):2137–2143. doi:10.1021/ma052539t
19. Fang FF, Kim JH, Choi HJ, Kim CA (2009) Synthesis and electrorheological response of nanosized Laponite stabilized poly(methyl methacrylate) spheres. Colloid Polym Sci 287(6):745–749
20. Liu YD, Zhang WL, Choi HJ (2012) Pickering emulsion polymerization of core-shell-structured polyaniline@SiO 2 nanoparticles and their electrorheological response. Colloid Polym Sci 290(9):855–860
21. Crevecoeur JJ, Nelissen L, Lemstra PJ (1999) Water expandable polystyrene (WEPS): Part 1. Strategy and procedures. Polymer 40(13):3685–3689. doi:10.1016/S0032-3861(98)00617-X
22. Snijders Emile A, Nelissen L, Lemstra Piet J (2006) Water expandable polystyrene (WEPS): Part 4. Synthesis of the water expandable blend of polystyrene and poly(2,6- dimethyl-1,4-phenylene ether). e-Polymers, vol 6. doi:10.1515/epoly.2006.6.1.994
23. Shen J, Cao X, James Lee L (2006) Synthesis and foaming of water expandable polystyrene–clay nanocomposites. Polymer 47(18): 6303–6310. doi:10.1016/j.polymer.2006.06.068
24. Crevecoeur JJ, Nelissen L, Lemstra PJ (1999) Water expandable polystyrene (WEPS): Part 2. In situ synthesis of (block) copolymer surfactants. Polymer 40(13):3691–3696. doi:10.1016/S0032-3861(98)00619-3
25. Pallay J, Kelemen P, Berghmans H, Van Dommelen D (2000) Expansion of polystyrene using water as the blowing agent. Macromol Mater Eng 275(1):18–25. doi:10.1002/(sici)1439-2054(20000201)275:1<18::aid-mame18>3.0.co;2-3
26. Amiri R-SN, Qazvini NT, Sanjani NS (2009) Water expandable polystyrene-organoclay nanocomposites: Role of clay and its dispersion state. J Macromol Sci B 48(5):955–966. doi:10.1080/00222340903032474
27. Garti N (1997) Progress in stabilization and transport phenomena of double emulsions in food applications. LWT Food Sci Technol 30(3): 222–235. doi:10.1006/fstl.1996.0176
28. Ma X, Jian R, Chang PR, Yu J (2008) Fabrication and characterization of citric acid-modified starch nanoparticles/plasticized-starch composites. Biomacromolecules 9(11):3314–3320. doi:10.1021/bm800987c
29. Fang JM, Fowler PA, Tomkinson J, Hill CAS (2002) The preparation and characterisation of a series of chemically modified potato starches. Carbohydr Polym 47(3):245–252. doi:10.1016/S0144-8617(01)00187-4
30. Putaux J-L, Molina-Boisseau S, Momaur T, Dufresne A (2003) Platelet nanocrystals resulting from the disruption of waxy maize starch granules by acid hydrolysis. Biomacromolecules 4(5):1198–1202. doi:10.1021/bm0340422
31. Huang M-F, Yu J-G, Ma X-F (2004) Studies on the properties of Montmorillonite-reinforced thermoplastic starch composites. Polymer 45(20):7017–7023. doi:10.1016/j.polymer.2004.07.068
32. van Soest JJG, Vliegenthart JFG (1997) Crystallinity in starch plastics: consequences for material properties. Trends Biotechnol 15(6): 208–213. doi:10.1016/S0167-7799(97)01021-4
33. Ma X, Yu J, Wang N (2008) Glycerol plasticized-starch/multiwall carbon nanotube composites for electroactive polymers. Compos Sci Technol 68(1):268–273. doi:10.1016/j.compscitech.2007.03.016
34. Zobel HF, Young SN, Rocca LA (1988) Starch gelatinization: An X-ray diffraction study. Cereal Chem 65(6):4
35. Xie X, Liu Q, Cui SW (2006) Studies on the granular structure of resistant starches (type 4) from normal, high amylose, and waxy cornstarch citrates. Food Res Int 39(3):332–341. doi:10.1016/j.foodres.2005.08.004
36. Pallay J, Berghmans H (2002) Water-blown expandable polystyrene. Improvement of the compatibility of the water carrier with the polystyrene matrix by In Situ grafting Part I. Mechanism of free radical grafting. Cell Polym 21(1):1–18
37. Aveyard R, Binks BP, Clint JH (2003) Emulsions stabilized solely by colloidal particles. Adv Colloid Interf Sci 100–102(SUPPL):503–546
38. Andresen M, Stenius P (2007) Water-in-oil emulsions stabilized by hydrophobized microfibrillated cellulose. J Dispers Sci Technol 28(6):837–844
39. Vaidya UR, Bhattacharya M (1994) Properties of blends of starch and synthetic polymers containing anhydride groups. J Appl Polym Sci 52(5):617–628. doi:10.1002/app.1994.070520505
40. Chauhan GS, Guleria LK, Misra BN, Kaur I (1999) Polymers from renewable resources. II. A study in the radio chemical grafting of poly(styrene-alt-maleic anhydride) onto cellulose extracted from pine needles. J Polym Sci A Polym Chem 37(12):1763–1769. doi:10.1002/(sici)1099-0518(19990615)37:12<1763::aid-pola5>3.0.co;2-s
41. Bastos DC, Santos AEF, da Silva MLVJ, Simão RA (2009) Hydrophobic cornstarch thermoplastic films produced by plasma treatment. Ultramicroscopy 109(8):1089–1093. doi:10.1016/j.ultramic.2009.03.031
42. Midmore BR (1999) Effect of aqueous phase composition on the properties of a silica-stabilized w/o emulsion. J Colloid Interface Sci 213(2):352–359. doi:10.1006/jcis.1999.6108
43. Binks BP, Lumsdon SO (2000) Catastrophic phase inversion of water-in-oil emulsions stabilized by hydrophobic silica. Langmuir 16(6):2539–2547. doi:10.1021/la991081j
44. Binks BP, Whitby CP (2004) Silica particle-stabilized emulsions of silicone oil and water: aspects of emulsification. Langmuir 20(4): 1130–1137. doi:10.1021/la0303557
45. Binks BP, Philip J, Rodrigues JA (2005) Inversion of silica-stabilized emulsions induced by particle concentration. Langmuir 21(8):3296–3302. doi:10.1021/la046915z
46. Abismaïl B, Canselier JP, Wilhelm AM, Delmas H, Gourdon C (1999) Emulsification by ultrasound: drop size distribution and stability. Ultrason Sonochem 6(1–2):75–83. doi:10.1016/S1350-4177(98)00027-3
47. Behrend O, Ax K, Schubert H (2000) Influence of continuous phase viscosity on emulsification by ultrasound. Ultrason Sonochem 7(2): 77–85. doi:10.1016/S1350-4177(99)00029-2
48. Das AK, Mukesh D, Swayambunathan V, Kotkar DD, Ghosh PK (1992) Concentrated emulsions. 3. Studies on the influence of continuous-phase viscosity, volume fraction, droplet size, and temperature on emulsion viscosity. Langmuir 8(10):2427–2436
49. Huang X, Kakuda Y, Cui W (2001) Hydrocolloids in emulsions: particle size distribution and interfacial activity. Food Hydrocoll 15(4–6):533–542. doi:10.1016/S0268-005X(01)00091-1
50. Yan N, Masliyah JH (1995) Characterization and demulsification of solids-stabilized oil-in-water emulsions Part 1. Partitioning of clay particles and preparation of emulsions. Colloids Surf A Physicochem Eng Asp 96(3):229–242. doi:10.1016/0927-7757(94)03058-8
51. Binks BP, Clint JH, Dyab AKF, Fletcher PDI, Kirkland M, Whitby CP (2003) Ellipsometric study of monodisperse silica particles at an oil–water interface. Langmuir 19(21):8888–8893. doi:10.1021/la035058g
52. Raghavan SR, Walls HJ, Khan SA (2000) Rheology of silica dispersions in organic liquids: new evidence for solvation forces dictated by hydrogen bonding. Langmuir 16(21):7920–7930. doi:10.1021/la991548q
53. Raghavan SR, Khan SA (1995) Shear-induced microstructural changes in flocculated suspensions of fumed silica. J Rheol 39(6): 1311–1325